FUB-HEP-91-1

FUB-HEP/91-1

Polarization phenomena and color magnetic effects in large-angle elastic proton-proton scattering §

Cai Xu *, Meng Ta-chung, Zhou Zhi-ning** and Zhou Zhuo-mei***

Institut für theoretische Physik

Freie Universität Berlin

Berlin, Germany

Ryk 363

§ Supported in part by Deutsche Forschungsgemeinschaft (me 470/5-2)

* On leave from Hua-Zhong Normal University, Wuhan, China

** On leave from Peking University, Beijing, China

*** On leave from Hua-Zhong University for Science and Technology, Wuhan, China

Abstract

It is shown that the striking features of the polarization data for large-angle elastic proton-proton scattering can be understood in the QCD framework, provided that the effects caused by the color-currents in polarized protons are taken into account. The color effects are treated phenomenologically at the hadronic level, where quantitative calculations are performed. The results obtained in this and in the previous paper strongly suggest the following: In collision processes in which the projectile- and the target-hadron get extremely close to each other (at least partial overlap in space) the bindings between the constituents — in particular the color magnetic forces between the constituents of one hadron and those of the other — are not negligible.

I. Introduction

It has now become more and more evident[1] that spin effects in high-energy collisions play a significant role in understanding hadronic phenomena. Besides the recent EMC muon-proton experiment[2] which triggered the "spin crisis"[1], a large number of other beautiful polarization experiments[1,3–9] have been performed since the beginning of the 1970's among which the following observations[3–9] made in high-energy large-momentum-transfer proton-proton elastic scattering processes are of particular interest. It is because these experiments are conceptually so simple, and the obtained data are so much different from the well-known[10] QCD predictions. In fact, the results of these experiments have been a standing challenge to the theorists already for manny years.[1,3–10]

The spin analyzing power A has been measured[3,4,5,9] up to incident momentum $p_{lab} = 28$ GeV/c using polarized targets and unpolarized beams. The transverse momenta ($p_\perp$) of the scattering protons in these experiments are large (up to $p_\perp^2 \approx 7\ (GeV/c)^2$). It is observed (Cf. Fig. 1, here, only the data at the two highest incident energies are shown.) that A is very much different from zero for $p_\perp^2 > 4\ (GeV/c)^2$, it increases dramatically in this region, and reaches more than 20% at $p_\perp^2 \approx 7\ (GeV/c)^2$). These "very non-zero values"[3] have attracted much attention, because it is known[10] that A must be zero wherever perturbative QCD is applicable. We recall that the analyzing power A is defined as

$$A = -\frac{1}{P_T}\,\frac{N(\uparrow) - N(\downarrow)}{N(\uparrow) + N(\downarrow)}\,, \tag{1.1}$$

and it is obtained from the measurements of the normalized event rates $N(i)(i = \uparrow$ or $\downarrow)$ of the transverely polarized target. Here, P_T is the magnitude of the target polarization; and the Basel convention is used in the definition of A (and thus the minus sign occurs because the forward proton in this experiment scattering to the right).[4,5]

Furthermore, the large $p_\perp^2$ behaviour of spin-spin correlations has been studied[3,6–9] up to incident momentum $p_{lab} = 18.5\ GeV/c$. In these experiments, transversely polarized ($i = \uparrow$ or

$\downarrow$) beam and transversely polarized ($j = \uparrow$ or $\downarrow$) target have been used and the normalized event rates $N(ij)$ have been measured. From these measurements the $p_\perp^2$-dependence of the spin-spin correlation parameter,

$$A_{nn} = \frac{1}{P_B P_T} \frac{N(\uparrow\uparrow) - N(\uparrow\downarrow) - N(\downarrow\uparrow) + N(\downarrow\downarrow)}{N(\uparrow\uparrow) + N(\uparrow\downarrow) + N(\downarrow\uparrow) + N(\downarrow\downarrow)} \tag{1.2}$$

has been obtained. Here, P_B and P_T are respectively the beam and target polarization. It is observed that A_{nn} depends strongly on the transverse momentum of the scattered proton. See Fig. 2. (Also here only the data at the two highest incident energies are shown.). Particularly striking is obviously the dramatic increase between $p_\perp^2 = 3$ and 5 $(GeV/c)^2$ at incident energy $p_{lab} = 11.75\ GeV/c$.

We recall that the above-mentioned $p_\perp^2$-dependence in the polarization data are not the only striking features of the large angle elastic proton-proton scattering data which have received much attention in the past. In fact, it is known[11] — already in the 1960's — that the differential cross sections $d\sigma/dt$ (t is the invariant momentum transfer) at fixed energies has a significant $p_\perp^2$-dependence. It decreases extremely fast with increasing $p_\perp^2$. The $d\sigma/dt$ data at $p_{lab} = 12\ GeV/c$ and that at $p_{lab} = 24\ GeV/c$, where most of the present polarization data on A and A_{nn} are taken, are shown in Fig. 3.

In an earlier paper,[12] we discussed the possible implications of the data on analyzing power,[3,4,5] and showed that the observed facts can be qualitatively understood in terms of the following picture:[13]

(i) Hadrons are spatially extended objects, and hadronic interactions are short ranged. Such a collision process between two hadrons (P and T say) can take place only when they are so close to each other that they partially overlap in space.

(ii) The constituents of the hadrons are quarks and gluons which carry color charges.

(iii) The color charges in a polarized proton rotate about the polarization axis.

The key idea of that paper is extremely simple, and it is based on an electromagnetic analog: Color charges rotating about the polarization axis of the target proton T are nothing else but axial

symmetric color currents which induce color magnetic fields. The projectile proton P is just another system of color charges which, in this scattering process, move with high velocity perpendicular to the polarization axis of T. Hence, the direction of the induced (color magnetic) field strength is expected to have an influence on the motion of P when the two colliding systems P and T get so close to each other that they partially overlap. The obtained result suggests that the influence is considerably large; and it shows that the proposed picture is able to give a qualitative description of the existing analyzing power data.

Encouraged by this result, we ask ourselves the following question: Is it possible to *quantify* this physical picture such that, not only the data on analyzing power but also those on *other* characteristic features of such scattering processes can be described in a *quantitative* way. Such an attempt has been made at the hadronic level. We are aware of the fact that a more straight-forward way would be a quantitative calculation at the quark-level — in terms of perturbative QCD. We did not choose such an approach for the following reasons: First, it is not clear to us whether the perturbative QCD is applicable — especially in those kinematical regions in which the above-mentioned experimental observations are made. Second, even if we *assume* that perturbative QCD *can be* applied in these cases, a calulation of this kind is obviously beyond the scope of non-experts in Computational Physics. (It is known[14] for example, that a perturbative QCD calculation to the 4th order in α_S for an exclusive meson-baryon scattering — which is considerably less complicated than that for baryon-baryon scattering — requires the evaluation of 33 helicity amplitudes each of which has 2195 distinct $0(\alpha_s^4)$ Feynmann diagrams !)

The formulism and the result of our quantitative description are presented in Sections III and IV. The relevant kinematics is discussed in Section II.

II Kinematical preliminaries

Nucleon-nucleon elastic scattering at relativistic energies has been extensively studied in the past.[15] It is well-known that, at least for the discussion of its kinematical aspects, the helicity formulism is very useful. We adopt this formalism and describe the elastic proton-proton scattering processes in the center-of-mass system by a matrix ϕ in spin space. The matrix is defined in such a way that for unpolarized beam and target the invariant differential cross-section $d\sigma/dt$ is given by[16]

$$\frac{d\sigma}{dt} = \frac{1}{4} \sum_{\lambda_1^i, \lambda_2^i, \lambda_1^f, \lambda_2^f} |\langle \lambda_1^f \lambda_2^f | \phi(p,\theta) | \lambda_1^i \lambda_2^i \rangle|^2. \tag{2.1}$$

Here, λ_1^i, λ_2^i are the helicities of initial and λ_1^f, λ_2^f are those of the final state. The matrix is a function of the c.m.s. momentum p and the c.m.s. scattering angle θ. Recall that t, the invariant momentum transfer is related to p and θ by $t = -4p^2 \sin^2(\theta/2)$. The helicity amplitudes are related to the usual[17] Feynman amplitudes $\mathcal{T}_{fi}$ for this process in the following way:[18]

$$\mathcal{T}_{fi} = \frac{4\sqrt{\pi p^2 (p^2 + m^2)}}{m^2} \langle \lambda_1^f \lambda_2^f | \phi(p,\theta) | \lambda_1^i, \lambda_2^i \rangle, \tag{2.2}$$

where m is the proton mass. (Here, we adopt the definition used by Goldberger et al.[17] where $\mathcal{T}_{fi}$ is related to the scattering matrix S as follows: $S \equiv 1 + iR$;
$\langle f|R|i\rangle \equiv (2\pi)^4 \delta^4(p_1^i + p_2^i - p_1^f - p_2^f) N \mathcal{T}_{fi}$; $N \equiv m^2 (2\pi)^{-6} (E_1^i E_2^i E_1^f E_2^f)^{-1/2}$; $E_1^i \equiv (|\vec{p}_1^i|^2 + m^2)^{1/2}$, similarly for E_2^i, E_1^f, E_2^f; p_1^i, p_2^i and p_1^f, p_2^f are the 4-momenta of the protons in the initial and the final states respectively.) For this scattering process, there are five independent helicity amplitudes:

$$\phi_1 = \langle ++ | \phi(p,\theta) | ++ \rangle, \qquad \triangle\lambda = 0, \tag{2.3}$$

$$\phi_2 = \langle ++ | \phi(p,\theta) | -- \rangle, \qquad \triangle\lambda = 2, \tag{2.4}$$

$$\phi_3 = \langle +- | \phi(p,\theta) | +- \rangle, \qquad \triangle\lambda = 0, \tag{2.5}$$

$$\phi_4 = \langle +- | \phi(p,\theta) | -+ \rangle, \qquad \triangle\lambda = 0, \tag{2.6}$$

$$\phi_5 = \langle ++ | \phi(p,\theta) | +- \rangle, \qquad \triangle\lambda = 1. \tag{2.7}$$

Here, the signs + and − stand for +1/2 and −1/2 respectively. The total change in helicity in a given amplitude, $\Delta\lambda$, is also indicated. In terms of these five amplitudes, the measured quantities $d\sigma/dt$ (the differential cross-section averaged over all possible initial spin states and summed over all final spin states; see Eq. 2.1), A (the analyzing power; see in Eq. 1.1) and A_{nn} (the spin-spin correlation parameter; see in Eq. 1.2) are related to one another through

$$\frac{d\sigma}{dt} = \frac{1}{2}\Big[|\phi_1|^2 + |\phi_2|^2 + |\phi_3|^2 + |\phi_4|^2 + 4|\phi_5|^2\Big], \tag{2.8}$$

$$A\frac{d\sigma}{dt} = -Im\Big[(\phi_1 + \phi_2 + \phi_3 - \phi_4)\phi_5^*\Big], \tag{2.9}$$

$$A_{nn}\frac{d\sigma}{dt} = Re\Big[\phi_1\phi_2^* - \phi_3\phi_4^* + 2|\phi_5|^2\Big]. \tag{2.10}$$

For discussions on the dynamical aspects of this scattering process it is more convenient to use another set of five independent amplitudes: f_S, f_V, f_T, f_A and f_P. (Note that, since we only discuss proton-proton elastic scattering in this paper, we omit in $f_\alpha, \alpha = S,V,T,A,P$ and in $\phi_i, i = 1,2,3,4,5$ the isospin-indices.). These amplitudes are functions of the invariant variables $s = (p_1^i + p_2^i)^2$, $t = (p_1^f - p_1^i)^2$, $u = (p_2^f - p_1^i)^2$, where $s + t + u = 4m^2$. They are associated with the standard "Fermi covariants":

$$S = \bar{u}(p_1^f)u(p_1^i)\bar{u}(p_2^f)u(p_2^i) \tag{2.11}$$

$$V = \bar{u}(p_1^f)\gamma_\mu u(p_1^i)\bar{u}(p_2^f)\gamma^\mu u(p_2^i) \tag{2.12}$$

$$T = \frac{1}{2}\bar{u}(p_1^f)\sigma_{\mu\nu}u(p_1^i)\bar{u}(p_2^f)\sigma^{\mu\nu}u(p_2^i) \tag{2.13}$$

$$A = \bar{u}(p_1^f)\gamma_5\gamma_\mu u(p_1^i)\bar{u}(p_2^f)\gamma_5\gamma^\mu u(p_2^i) \tag{2.14}$$

$$P = \bar{u}(p_1^f)\gamma_5(p_1^i)\bar{u}(p_2^f)\gamma_5 u(p_2^i) \tag{2.15}$$

used by Goldberger et al. (GGMW) and others[15] such that the scattering amplitude $\mathcal{T}_{fi}$ in Eq. (2.2) can be rewritten as:

$$\begin{aligned}\mathcal{T}_{fi} = &\Big[f_S(s,t,u)S + f_V(s,t,u)V + f_T(s,t,u)T + f_A(s,t,u)A + f_P(s,t,u)P\Big] \\ &- \Big[f_S(s,u,t)\tilde{S} + f_V(s,u,t)\tilde{V} + f_T(s,u,t)\tilde{T} + f_A(s,u,t)\tilde{A} + f_P(s,u,t)\tilde{P}\Big].\end{aligned} \tag{2.16}$$

Here, $\sigma_{\mu\nu} \equiv i(\gamma_\mu\gamma_\nu - \gamma_\nu\gamma_\mu)/2, \gamma_5 \equiv i\gamma_0\gamma_1\gamma_2\gamma_3 \equiv \gamma^5, u(p_1^i)$ is the Dirac spinor for the incoming point-like proton of mass m, momentum p_1^i and helicity λ_1^i, and $\bar{u}(p_1^f)$ is that for the outgoing proton with momentum p_1^f and helicity λ_1^f, etc. The Fermi covariant $\tilde{S}$ is obtained by interchanging, in the expression (2.11) for S, $\bar{u}(p_1^f)$ and $\bar{u}(p_2^f)$; $\tilde{V}, \tilde{T}, \tilde{A}$ and $\tilde{P}$ are obtained in a similar way. This set of covariants is related to the set S, V, T, A, P by the well-known[19] formula:

$$\begin{pmatrix} \tilde{S} \\ \tilde{V} \\ \tilde{T} \\ \tilde{A} \\ \tilde{P} \end{pmatrix} = \frac{1}{4} \begin{pmatrix} 1 & 1 & 1 & 1 & 1 \\ 4 & -2 & 0 & 2 & -4 \\ 6 & 0 & -2 & 0 & 6 \\ 4 & 2 & 0 & -2 & -4 \\ 1 & -1 & 1 & -1 & 1 \end{pmatrix} \begin{pmatrix} S \\ V \\ T \\ A \\ P \end{pmatrix}. \tag{2.17}$$

The function $f_\alpha(s,u,t)$ is obtained by interchanging t and u in $f_\alpha(s,t,u)$. The requirements imposed by Pauli principle for elastic proton-proton scattering are always satisfied by the expression for $\mathcal{T}_{fi}$ given in Eq. (2.16) — independent of the explicit forms of the functions f_S, f_V, f_T, f_A and f_P. Note in particular that, in the center-of-mass frame, the interchange of t and u corresponds to the interchange of the scattering angle θ and the angle $\pi - \theta$. The relationship between these five amplitudes and the five helicity amplitudes $\phi_1, \phi_2, \phi_3, \phi_4$ and ϕ_5 can be obtained by comparing Eq.(2.2) with Eq. (2.16) The result is:

$$\begin{pmatrix} \phi_1 \\ \phi_2 \\ \phi_3 \\ \phi_4 \\ \phi_5 \end{pmatrix} = \frac{1}{4\sqrt{\pi}\sqrt{s(s-4m^2)^3}} \left(K \begin{pmatrix} f_S(s,t,u) \\ f_V(s,t,u) \\ f_T(s,t,u) \\ f_A(s,t,u) \\ f_P(s,t,u) \end{pmatrix} + L \begin{pmatrix} f_S(s,u,t) \\ f_V(s,u,t) \\ f_T(s,u,t) \\ f_A(s,u,t) \\ f_P(s,u,t) \end{pmatrix} \right) \tag{2.18}$$

Here, K and L are 5×5 matrices. They can be written in the following way, where the (t,u) symmetry can be explicitly seen:

$$K = \begin{pmatrix} -4m^2 & -(2s-4m^2) & 4m^2 & 2s-4m^2 & 0 \\ 0 & 0 & -2(2s-4m^2) & -2(4m^2) & 0 \\ -4m^2 & -(2s-4m^2) & -4m^2 & -(2s-4m^2) & 0 \\ 0 & 0 & 0 & 0 & 0 \\ 0 & 0 & 0 & 0 & 0 \end{pmatrix} u +$$

$$+\begin{pmatrix} 0 & -2(s-4m^2) & 2(4m^2) & 2s & 0 \\ s & 4m^2 & -(2s-4m^2) & -4m^2 & s-4m^2 \\ 0 & 0 & 0 & 0 & 0 \\ -s & -4m^2 & -4m^2 & -4m^2 & s-4m^2 \\ 0 & 0 & 0 & 0 & 0 \end{pmatrix} t+$$

$$+\begin{pmatrix} 0 & 0 & 0 & 0 & 0 \\ 0 & 0 & 0 & 0 & 0 \\ 0 & 0 & 0 & 0 & 0 \\ 0 & 0 & 0 & 0 & 0 \\ -2m\sqrt{s} & -2m\sqrt{s} & -2m\sqrt{s} & -2m\sqrt{s} & 0 \end{pmatrix} \sqrt{ut} \tag{2.19}$$

$$L = \begin{pmatrix} -4m^2 & -(2s-4m^2) & 4m^2 & 2s-4m^2 & 0 \\ 0 & 0 & -2(2s-4m^2) & -2(4m^2) & 0 \\ 0 & 0 & 0 & 0 & 0 \\ 4m^2 & 2s-4m^2 & 4m^2 & 2s-4m^2 & 0 \\ 0 & 0 & 0 & 0 & 0 \end{pmatrix} t+$$

$$+\begin{pmatrix} 0 & -2(s-4m^2) & 2(4m^2) & 2s & 0 \\ s & 4m^2 & -(2s-4m^2) & -4m^2 & s-4m^2 \\ s & 4m^2 & 4m^2 & 4m^2 & -(s-4m^2) \\ 0 & 0 & 0 & 0 & 0 \\ 0 & 0 & 0 & 0 & 0 \end{pmatrix} u+$$

$$+\begin{pmatrix} 0 & 0 & 0 & 0 & 0 \\ 0 & 0 & 0 & 0 & 0 \\ 0 & 0 & 0 & 0 & 0 \\ 0 & 0 & 0 & 0 & 0 \\ 2m\sqrt{s} & 2m\sqrt{s} & 2m\sqrt{s} & 2m\sqrt{s} & 0 \end{pmatrix} \sqrt{ut} \tag{2.20}$$

III A phenomenological approach at the hadronic level

After the kinematical preliminary we are now ready to continue our discussion on the problems mentioned in Sections I. We present the general formalism of a phenomenological approach to elastic pp scattering here, and discuss its application to large-angle processes in Section IV.

The proposed phenomenological approach is made at the hadronic level in terms of relativistic quantum mechanics. In this formalism, each of the two protons taking part in an elastic scattering process is described by a single-particle wave functions $\Psi(x|1)$ or $\Psi(x|2)$ (of the space-time 4-vector x). Since, in the interaction region, each of them can be considered as moving in the field generated by the other, these wave functions are assumed to satisfy the following coupled integrodifferential equations

$$(i\gamma^\mu \partial_\mu - m)\Psi(x|1) = I(x|2)\Psi(x|1), \tag{3.1}$$

$$(i\gamma^\mu \partial_\mu - m)\Psi(x|2) = I(x|1)\Psi(x|2). \tag{3.2}$$

Here, γ^μ $(\mu = 0,1,2,3)$ are the Dirac matrices, $\partial_\mu \equiv \partial/\partial x^\mu$, m is the proton mass, and the operators

$$I(x|2) = \sum_\alpha O_\alpha \int d^4x' c_\alpha(x'-x)\Big[\bar{\Psi}(x'|2) - \bar{\Psi}(x'|1)\Big] O_\alpha \Psi(x'|2), \tag{3.3}$$

$$I(x|1) = \sum_\alpha O_\alpha \int d^4x' c_\alpha(x'-x)\Big[\bar{\Psi}(x'|1) - \bar{\Psi}(x'|2)\Big] O_\alpha \Psi(x'|1) \tag{3.4}$$

describe the interaction between the two colliding protons. The method of describing a system of interacting particles in terms of single-particle wave functions which satisfy a set of coupled integrodifferential equations is not new. In fact, the spirit of this formalism is the same as that of Hartree-Fock method[20] in Atomic Physics, where the motion of each electron in an atom (with more than one electrons) is regarded as being in motion in the "self-consistent field" due to the nucleus together with other electrons. Furthermore (as can be seen in more detail later on), this formalism has also much in common with the propagator theory[21] of Quantum Electrodynamics. Formally, the basic difference between the afore-mentioned theories and our approach is that,

in the latter, there are in general five different types of interactions — namely the scalar, the vector, the tensor, the axial vector, and the pseudoscalar type of interactions. This is because, in our attempt of describing the color effects at the hadronic level, we take the following facts into account: The effects of color-electric and the color-magnetic interactions between the constituents of the colliding hadrons depend in general on the structures of the hadrons as well as on the details of the reaction mechanisms. Without such detailed information we have to make guesses as to how the color effects manifest themselves at the hadronic level. In doing this, it is helpful to classify the possible interactions according to the transformation properties of the corresponding bilinear forms $\bar{\Psi}O_\alpha\Psi$ (where $\bar{\Psi}$ is the adjoint of Ψ) under Lorentz-transformation. The operator O_α, where $\alpha = S, V, T, A, P$, stands for $\mathbf{1}$ (the unit 4×4 matrix), $\gamma^\mu, \sigma^{\mu\nu}/\sqrt{2}, \gamma^\mu\gamma_5$ and γ_5 respectively. All the c_α's in Eqs. (3.3) and(3.4) are c-number scalar functions. The function c_α will hereafter be called the "coupling-function of the α-type"; and all the c_α's are taken to be even functions of $x' - x$ in order to guarantee invariance under translation and reflection in space-time.

Approximative solutions of Eqs. (3.1)-(3.4) can be obtained by successive iteration, provided that the coupling functions $c_\alpha(\alpha = S, V, T, A, P)$ are known. That is, these equations can be rewritten as:

$$(i\gamma^\mu\partial_\mu - m)\Psi_{n+1}(x|1) = I_n(x|2)\Psi_{n+1}(x|1), \tag{3.5}$$

$$(i\gamma^\mu\partial_\mu - m)\Psi_{n+1}(x|2) = I_n(x|1)\Psi_{n+1}(x|2), \tag{3.6}$$

Here, Ψ_n is the nth-order-approximation of Ψ, with $\Psi_o \equiv \psi$, where $(i\gamma^\mu\partial_\mu - m)\psi = 0$; and $\bar{\Psi}_n$ is the corresponding nth-order approximation of $\bar{\Psi}$. The operators $I_n(x|2)$ and $I_n(x|1)$ are respectively the nth-order-approximations of $I(x|1)$ and $I(x|2)$ which can be expressed in terms of $U_n^{(\alpha)}$, "the effective potentials of order n":

$$I_n(x|2) = \sum_\alpha O_\alpha \, [U_n^{(\alpha)}(x|2,2) - U_n^{(\alpha)}(x|1,2)], \tag{3.7}$$

$$I_n(x|1) = \sum_\alpha O_\alpha \, [U_n^{(\alpha)}(x|1,1) - U_n^{(\alpha)}(x|2,1)]. \tag{3.8}$$

In accordance with the Eqs. (3.3) - (3.8), the effective potentials $U_n^{(\alpha)}(x|j,k)$, where j and k can be either 1 or 2, are given by

$$U_n^{(\alpha)}(x|j,k) = \int d^4x' c_\alpha(x'-x)\bar{\Psi}_n(x'|j)O_\alpha\Psi_n(x'|k). \tag{3.9}$$

We note: Since all the c_α's are scalar functions, the transformation property of $U_n^{(\alpha)}$ is simply that of $\bar{\Psi}_n O_\alpha \Psi_n$. Hence, we call $U_n^{(S)} \equiv U_{nS}$, $U_n^{(V)} \equiv U_{nV} \equiv \{U_{nV}^\mu\}$, $U_n^{(T)} \equiv U_{nT} \equiv \{U_{nT}^{\mu\nu}\}$, $U_n^{(A)} \equiv U_{nA} \equiv \{U_{nA}^\mu\}$, $U_n^{(P)} \equiv U_{nP}$, $(\mu,\nu = 0,1,2,3)$, respectively the scalar, the vector, the tensor, the axial-vector, and the pseudoscalar effective potentials of the nth order.

From Eq. (3.9), we see that the components of the zeroth order effective potentials can be expressed in terms of ψ and $\bar{\psi}$, the solutions of the free Dirac equations. They are:

$$U_{0S}(x|j,k) = \int d^4x' c_S(x'-x)\bar{\psi}(x'|j)\psi(x'|k), \tag{3.10a}$$

$$U_{0V}^\mu(x|j,k) = \int d^4x' c_V(x'-x)\bar{\psi}(x'|j)\gamma^\mu\psi(x'|k), \tag{3.10b}$$

$$U_{0T}^{\mu\nu}(x|j,k) = \int d^4x' c_T(x'-x)\bar{\psi}(x'|j)\sigma^{\mu\nu}/\sqrt{2}\psi(x'|k), \tag{3.10c}$$

$$U_{0A}^\mu(x|j,k) = \int d^4x' c_A(x'-x)\bar{\psi}(x'|j)\gamma_5\gamma^\mu\psi(x'|k), \tag{3.10d}$$

$$U_{0P}(x|j,k) = \int d^4x' c_P(x'-x)\bar{\psi}(x'|j)\gamma_5\psi(x'|k). \tag{3.10e}$$

This means, for a given set of coupling functions $c_\alpha(\alpha = S,V,T,A,P)$, the zeroth-order interactions $I_0(x|1)$ and $I_0(x|2)$ can be obtained in the following way: Insert the initial and the final state wave functions for the free protons [with quantum numbers $(p_1^i,\lambda_1^i),(p_2^i,\lambda_2^i)$ and $(p_1^f,\lambda_1^f),(p_2^f,\lambda_2^f)$ respectively] into Eqs. (3.10a)-(3.10e) to determined $U_{0S}(x|j,k),...,U_{0P}(x|j,k)$; and then insert these results into Eqs. (3.7) and (3.8) to obtain $I_0(x|1)$ and $I_0(x|2)$. We note in particular: This is why – and how – the interaction $I_0(x|1)$ and $I_0(x|2)$ depend on the polarizations of the initial state and those of the final states of the colliding protons.

The effective potentials of order n defined in Eq. (3.9), in particular the zeroth order approximations given in Eqs. (3.10a)-(3.10e) are closely related to the usual potentials in "direct" and

"exchange" processes. Let us, without restriction of generality, associate the final state described by (p_1^f, λ_1^f) with the initial state (p_1^i, λ_1^i) in the sense that they are taken to be the asymptotical limits of the same wave function which, at the space-time point x', is represented by $\Psi(x'|1)$ [and similarly (p_2^f, λ_2^f) with (p_2^i, λ_2^i) represented by $\Psi(x'|2)$]. Then, all the effective potentials $U_{0S}(x|j,k), ..., U_{0P}(x|j,k)$ with $j = k$ describe "direct scatterings" , while those with $j \neq k$ are responsible for the "exchange processes". To be more precise, while $U_{0\alpha}(x|2,2)$ is the zeroth-order α-type effective potential (at the space-time point x) generated by a proton described by all the wave functions with initial state (p_2^i, λ_2^i) and final state (p_2^f, λ_2^f) (at all possible space-time points x' over which we integrate), $U_{0\alpha}(x|1,2)$ is the corresponding "exchange potential" generated by a proton with initial state (p_2^i, λ_2^i) and final state (p_1^f, λ_1^f). This is illustrated in Fig. 4. In other words, while $U_{0\alpha}(x|2,2)$ causes the proton in initial state (p_1^i, λ_1^i) to enter the final state (p_1^f, λ_1^f), $U_{0\alpha}(x|1,2)$ is responsible for the effect that the proton in initial state (p_1^i, λ_1^i) to enter the final state (p_2^f, λ_2^f). Similarly for $U_{0\alpha}(x|1,1)$ and $U_{0\alpha}(x|2,1)$.

It should also be mentioned that $U_{0\alpha}(x|i,j)$ — in general $U_{n\alpha}(x|i,j)$ — are operators in Eqs. (3.5) and (3.6). In accordance with its definition, it yields its eigenvalue [which is $U_{0\alpha}(x|i,j)$, in general $U_{0\alpha}(x|i,j)$] when this operator is applied to a proton wave function, unless the wave function happens to be the one that generates this effective potential. In the latter case, it is zero, because we are not dealing with "self-interactions". It is clear that, after having solved Eqs. (3.5) and (3.6) for $n = 0$ and thus obtained $\Psi_1(x|1)$ and $\Psi_1(x|2)$, we can construct $I_1(x|1), I_1(x|2)$ in a similar way. Furthermore, similar interpretation is also possible for higher order approximations. This means, an adequate phenomenological description of the interaction between the protons in elastic proton-proton scattering can be achieved (step by step), provided that the five coupling functions $c_\alpha(\alpha = S, V, T, A, P)$ are known.

Hence, having this physical picture — together with the notion of effective potentials and the method of successive iteration — in mind, we can now proceed to write down the matrix element between the following two states: The initial state i, represented by the product of two single-particle positive energy solutions $\psi(x|i)\psi(x|i)$ of the free Dirac equation where the corresponding

momenta and helicities are (p_1^i, λ_1^i) and (p_2^i, λ_2^i); and the final state f, represented by the product $\bar{\psi}(x|1^f)\bar{\psi}(x|2^f)$ with the quantum numbers (p_1^f, λ_1^f) and (p_2^f, λ_2^f). In terms of the wave functions $\Psi(x|1)$ and $\Psi(x|2)$, which for $x_o \to -\infty$ reduce to $\psi(x|1)$ and $\psi(x|2)$ respectively, and the functions $I(x|2)$ and $I(x|1)$ defined in Eqs.(3.3) and (3.4), the scattering matrix element $\langle f|R|i\rangle$ which we mentioned in connection with $\mathcal{T}_{fi}$ in Eq. (2.2) can be expressed as follows:[22]

$$\begin{aligned}\langle f|R|i\rangle = \frac{1}{2}\int dx^4\Big[&\bar{\psi}(x|1^f)I(x|2^i)\Psi(x|1^i) + \bar{\psi}(x|2^f)I(x|2^i)\Psi(x|1^i)+ \\ &\bar{\psi}(x|2^f)I(x|1^i)\Psi(x|2^i) + \bar{\psi}(x|1^f)I(x|1^i)\Psi(x|2^i)\Big]\end{aligned} \tag{3.11}$$

As can be readily seen — from the definitions of $I(x|2^i)$ and $I(x|1^i)$ given in Eqs. (3.3) and (3.4) — that, in the integrand of Eq. (3.11), the first term is identical with the third, the second with the fourth. This is why a factor 1/2 has been introduced on the right-hand-side to avoid double-counting. It means, in the Born approximation, the scattering matrix element $\langle f|R|i\rangle^{Born}$ can be written as[23]

$$\begin{aligned}\langle f|R|i\rangle^{Born} &= \frac{1}{2}\int d^4x\Big[\bar{\psi}(x|1^f)I(x|2^i)\psi(x|1^i) + \bar{\psi}(x|2^f)I(x|2^i)\psi(x|1^i)+ \\ &\qquad \bar{\psi}(x|2^f)I(x|1^i)\psi(x|2^i) + \bar{\psi}(x|1^f)I(x|1^i)\psi(x|2^i)\Big] = \\ &= \frac{1}{2}\sum_\alpha\int d^4x\Big[\bar{\psi}(x|1^f)O_\alpha U_{0\alpha}(x|2^f,2^i)\psi(x|1^i) - \bar{\psi}(x|2^f)O_\alpha U_{0\alpha}(x|1^f,2^i)\psi(x|1^i)+ \\ &\qquad \bar{\psi}(x|2^f)O_\alpha U_{0\alpha}(x|1^f,1^i)\psi(x|2^i) - \bar{\psi}(x|1^f)O_\alpha U_{0\alpha}(x|2^f,1^i)\psi(x|2^i)\Big].\end{aligned} \tag{3.12}$$

As usual, we write the positive energy solution of the free Dirac equation for protons with given four-momentum $p^i \equiv (E^i, \vec{p}^i)$ and given helicity λ^i in the form

$$\psi(x|i) = \sqrt{\frac{m}{(2\pi)^3 E^i}}\; e^{-ip^i x} u_i(p^i), \tag{3.13}$$

Here, $\psi(x|i)$ stand for $\psi(x|1^i)$ or $\psi(x|2^i)$, and u_i is the corresponding positive-energy spinor with normalization $\bar{u}_i u_i = 1$. The final-state protons is correspondingly:

$$\bar{\psi}_f(x|f) = \sqrt{\frac{m}{(2\pi)^3 E^f}}\; e^{ip^f x}\bar{u}_f(p^f). \tag{3.14}$$

where $\bar{\psi}(x|f)$ can be either $\bar{\psi}(x|1^f)$ or $\bar{\psi}(x|2^f)$. We also introduce the Fourier transform, $g_\alpha(q)$, of the coupling functions $c_\alpha(x)$ for $\alpha = S, V, T, A$ and P:

$$c_\alpha(x) = (2\pi)^{-4} \int d^4q e^{-iqx} g_\alpha(q). \tag{3.15}$$

We now compare $\langle f|R|i\rangle^{Born}$ given in Eq.(3.12) with the general expression for $\langle f|R|i\rangle$ which leads to $\mathcal{T}_{fi}$ given in Eqs. (2.2) and (2.16). We identify the four-momenta p^i and p^f in Eqs. (3.13) and (3.14) respectively with p_1^i, p_2^i and p_1^f, p_2^f which appear in the bilinear covariants in Eqs. (2.11) - (2.15). We express the functions $\psi(x'|k)$ and $\bar{\psi}(x'|j)$ in Eqs. (3.10a) - (3.10e) in terms of the above-mentioned plane wave solutions of the Dirac equations with given four-momenta p_1^i, p_2^i and p_1^f, p_2^f and the corresponding spinors respectively. Here, we recall that the interchange of p_1^f and p_2^f and the corresponding helicities causes the interchange of the invariant variables t and u as well as the interchange of the two sets of covariants (S, V, T, A, P) and $(\tilde{S}, \tilde{V}, \tilde{T}, \tilde{A}, \tilde{P})$. We insert Eqs. (3.10a) - (3.10e), (3.13), (3.14), (3.15) and the corresponding expressions for $\psi(x|1^i), \psi(x|2^i), \bar{\psi}(x|1^f)$ and $\bar{\psi}(x|2^f)$ into Eq. (3.12); and carry out the integration. From this we obtain: $\langle f|R|i\rangle^{Born} = (2\pi)^4\delta^4(p_1^i + p_2^i - p_1^f - p_2^f) N \mathcal{T}_{fi}^{Born}$, where $N = (2\pi)^{-6} m^2 E^{-2}, E = (p^2 + m^2)^{1/2}$ and

$$\begin{aligned}\mathcal{T}_{fi}^{\text{Born}} = &\Big[g_S(s,t)S + g_V(s,t)V + g_T(s,t)T + g_A(s,t)A + g_P(s,t)P\Big] - \\ &\Big[g_S(s,u)\tilde{S} + g_V(s,u)\tilde{V} + g_T(s,u)\tilde{T} + g_A(s,u)\tilde{A} + g_P(s,u)\tilde{P}\Big],\end{aligned} \tag{3.16}$$

That is, on identifing this result with the general expression for $\mathcal{T}_{fi}$ given in Eq.(2.16), we see that, in Born approximation, the invariant amplitudes f_α $(\alpha = S, V, T, A, P)$, are simply:

$$f_\alpha(s,t,u) = g_\alpha(s,t), \tag{3.17}$$

$$f_\alpha(s,u,t) = g_\alpha(s,u), \tag{3.18}$$

where $t = (p_1^f - p_1^i)^2$ and $u = (p_2^f - p_1^i)^2$. We recall that the g_α is the 4-dimensional Fourier transform of the scalar function c_α of the space-time variable $x - x'$, and thus it is in general function of the invariant momentum transfer t or u as well as of the invariant total energy squared

s. We also recall that s, t and u can be expressed in terms of the c.m.s. momentum p and the c.m.s. scattering angle θ : $s = 4(p^2 + m^2)$, $t = -2p^2(1 - cos\theta)$, $u = -2p^2(1 + cos\theta)$.

Hence, the general conclusion we can now draw is the following: In the Born approximation, all the measurable quantities in elastic proton-proton scattering can be readily obtained, provided that the quantum numbers of the initial- and final state of the colliding protons are given and that the five coupling functions $c_\alpha(\alpha = S, V, T, A, P)$ are known.

It should be mentioned that the special case:

$$c_\alpha(x - x') = \delta(x^0 - x^{0'})\bar{c}_\alpha(|\vec{x} - \vec{x}'|), \qquad \alpha = S, T, V, A, P \tag{3.19}$$

in a given reference frame is of particular interest in practice, because (having the well-known Fermi-coupling as the limiting case of weak interaction in mind) instantaneous propagation of interaction is expected to be a good approximation when the impact parameter is very small (compared to the average size of the colliding hadrons) and thus the corresponding momentum transfer is relatively large. In this connection it is also useful to introduce $\bar{g}_\alpha$, the 3-dimensional Fourier transform of $\bar{c}_\alpha$

$$\bar{c}_\alpha(|\vec{x}|) = (2\pi)^{-3} \int d^3q e^{i\vec{q}\cdot\vec{x}} \bar{g}_\alpha(\vec{q}), \tag{3.20}$$

for $\alpha = S, T, V, A$ and P. Here, $q \equiv (q^0, \vec{q})$ is the four-momentum transfer.

In order to show what kind of a role coupling functions play in practice, a few illustrative examples may be helpful: In Example 1 we consider:

$$\begin{aligned} &\bar{c}_S(r) = \bar{c}_V(r) = \bar{c}_T(r) = \bar{c}_A(r) = 0, \\ &\bar{c}_P(r) = -\kappa e^{-\mu r}/r, \end{aligned} \tag{3.21}$$

where r stands for $|\vec{x}' - \vec{x}|$, κ and μ are positive real constants. The invariant amplitudes f_α in the

Born approximation can be readily evaluated. They are:

$$
\begin{aligned}
&f_\alpha(s,t,u) = f_\alpha(s,u,t) = 0, && \text{for } \alpha = S,V,T,A, \\
&f_P(s,t,u) = \frac{4\pi\kappa}{t-\mu^2}, && f_P(s,u,t) = \frac{4\pi\kappa}{u-\mu^2}.
\end{aligned}
\tag{3.22}
$$

This is obviously the one-pion-exchange contribution[24] to elastic proton-proton scattering, where μ is the pion mass, and κ is equal to the pion-proton coupling constant. In Example 2, we consider the case in which

$$
\begin{aligned}
&\bar{c}_S(r) = \bar{c}_T(r) = \bar{c}_A(r) = \bar{c}_P(r) = 0, \\
&\bar{c}_V(r) = \frac{e}{r},
\end{aligned}
\tag{3.23}
$$

where e is the electric charge. Here, the corresponding effective potentials in Born approximation are:

$$
\begin{aligned}
&U_{0S}(x|j,k) = U_{0T}^{\mu\nu}(x|j,k) = U_{0A}^{\mu}(x|j,k) = U_{0P}(x|j,k) = 0, \\
&U_{0V}^{\mu}(x|j,j) = -U_{0V}^{\mu}(x|j,k \neq j) = A^\mu(x),
\end{aligned}
\tag{3.24}
$$

where $j,k = 1,2$; and $A^\mu(x)$ is the electromagnetic potential.[25] That is, Eq.(3.10b) for $j = k$ is nothing else but the usual[21] relation between the four-potential $A^\mu(x)$ and the four-current density $\bar{\psi}(x'|j)\gamma^\mu\psi(x'|j)$. It shows in particular why and how the effective potentials depend on the initial and the final *spin-states* of the particle. In fact, on inserting Eqs. (3.23) (3.24) (3.19) into Eq. (3.10b) and on taking the non-relativistic limit, we obtain the usual spin-orbit and spin-spin interaction terms which appear in the Hamilton operator of such a scattering problem. Another well-known result which we explicitly see in this example is the following: In the ultra-relativistic limit, that is, in the high-energy limit where the mass of the colliding particles can be neglected, the helicity of each of the colliding objects is conserved.

As a further example, we consider the general case (in which all c_α's are different from zero) and compare the corresponding nonrelativistic limit with the (non-covariant) formulism discussed by Durand and Halzen.[15] In their formalism, the components of the various spin parameters are

referred to a set of axes specified by the unit vectors $\hat{\vec{\ell}}, \hat{\vec{q}}$ and $\hat{\vec{n}}$:

$$\vec{\ell} = \vec{p}^f + \vec{p}^i, \quad \hat{\vec{\ell}} = \frac{\vec{\ell}}{\ell}, \quad \ell = |\vec{\ell}|, \tag{3.25}$$

$$\vec{q} = \vec{p}^f - \vec{p}^i, \quad \hat{\vec{q}} = \frac{\vec{q}}{q}, \quad q = |\vec{q}|, \tag{3.26}$$

$$\vec{n} = \vec{\ell} \times \vec{q}, \quad \hat{\vec{n}} = \frac{\vec{n}}{n}, \quad n = |\vec{n}| = \ell q, \tag{3.27}$$

where $\vec{p}^i$ the initial, and $\vec{p}^f$ final momentum in the centre-of-mass system (thus $|\vec{p}^i| = |\vec{p}^f|$). Denoting the "large component" of the four-spinor $\psi(x|j)$ $(j = 1,2)$ by $\varphi(j)$, the non-relativistic limit of the scattering amplitude $\mathcal{T}_{fi}$ can be written in the following form

$$\begin{aligned}\mathcal{T}_{fi}^{NR} =& \mathcal{M}_0 \ \langle I_1\rangle\langle I_2\rangle + \mathcal{M}_1 \left[\langle I_1\rangle\langle\vec{\sigma}_2\rangle + \langle I_2\rangle\langle\vec{\sigma}_1\rangle\right]\cdot\hat{\vec{n}} + \\ &+ \mathcal{M}_2 \ \langle\vec{\sigma}_1\rangle\cdot\hat{\vec{n}} \ \langle\vec{\sigma}_2\rangle\cdot\hat{\vec{n}} + \mathcal{M}_3 \ \ \langle\vec{\sigma}_1\rangle\cdot\hat{\vec{q}} \ \langle\vec{\sigma}_2\rangle\cdot\hat{\vec{q}} + + \mathcal{M}_4 \ \ \langle\vec{\sigma}_1\rangle\cdot\hat{\vec{\ell}} \ \langle\vec{\sigma}_2\rangle\cdot\hat{\vec{\ell}}\end{aligned} \tag{3.28}$$

$$\langle I_j\rangle = \varphi_f^\dagger(j)\varphi_i(j), \tag{3.29}$$

$$\langle\vec{\sigma}_j\rangle = \varphi_f^\dagger(j)\vec{\sigma}\varphi_i(j) \tag{3.30}$$

$$\mathcal{M}_0 = \bar{g}_S + (1 + \frac{1}{2}\frac{\ell^2}{m^2})\bar{g}_V + \frac{1}{2}\frac{q^2}{m^2}\bar{g}_T \tag{3.31}$$

$$\mathcal{M}_1 = \frac{i}{4}\frac{\ell q}{m^2}\bar{g}_V + \frac{i}{2}\frac{\ell q}{m^2}\bar{g}_T \tag{3.32}$$

$$\mathcal{M}_2 = \frac{-1}{4}\frac{\ell^2}{m^2}\bar{g}_V + (2 + \frac{1}{2}\frac{\ell^2}{m^2})\bar{g}_T + (-1)\bar{g}_A \tag{3.33}$$

$$\mathcal{M}_3 = \frac{-1}{4}\frac{\ell^2}{m^2}\bar{g}_V + (2 + \frac{1}{2}\frac{\ell^2}{m^2})\bar{g}_T + (-1 + \frac{1}{4}\frac{q^2}{m^2})\bar{g}_A + \frac{-1}{4}\frac{q^2}{m^2}g_P \tag{3.34}$$

$$\mathcal{M}_4 = (2 + \frac{\ell^2}{m^2})\bar{g}_T + (-1)\bar{g}_A \tag{3.35}$$

$$\bar{g}_\alpha = \bar{g}_\alpha(q) = \int d^3r\bar{c}_\alpha(r)e^{-i\vec{q}\cdot\vec{r}} \qquad \alpha = S, V, T, A, P \tag{3.36}$$

That is, Eqs.(3.31)-(3.35) show whether/how the nonrelativistic limit of the S,V,T,A,P-couplings contribute to the Durand-Halzen amplitudes.[15] The relative importance of the different couplings

to the various polarization parameters is summarized in Table 1.

type of interaction	S	V	T	A	P	S	V	T	A	P
$\langle I_1\rangle\langle I_2\rangle$	$\surd$	$\surd$					$\surd$	$\surd$		
$[\langle I_1\rangle\langle\vec{\sigma}_2\rangle + \langle I_2\rangle\langle\vec{\sigma}_1\rangle]\cdot\hat{\vec{n}}$							$\surd$	$\surd$		
$\langle\vec{\sigma}_1\rangle\cdot\hat{\vec{\ell}}\,\langle\vec{\sigma}_2\rangle\cdot\hat{\vec{\ell}}$			$\surd$	$\surd$				$\surd$		
$\langle\vec{\sigma}_1\rangle\cdot\hat{\vec{q}}\,\langle\vec{\sigma}_2\rangle\cdot\hat{\vec{q}}$			$\surd$	$\surd$			$\surd$	$\surd$	$\surd$	$\surd$
$\langle\vec{\sigma}_1\rangle\cdot\hat{\vec{n}}\,\langle\vec{\sigma}_2\rangle\cdot\hat{\vec{n}}$			$\surd$	$\surd$			$\surd$	$\surd$		
order of magnitude			$0(1)$					$0(\frac{1}{m^2})$		

Table 1

Last but not least, it should be mention that, also in the ultra-relativistic limit, different types of couplings behave, in general, differently. One of the most interesting properties is the question whether/which coupling may cause helicity-flip. This question can be readily answered; the result is summarized in Table 2.

type of interaction	S	V	T	A	P
change in helicity	yes	no	yes	no	yes

Table 2

From these examples we see why it is useful to study the non-relativistic and the ultrarelativistic limits: They explicitly show which type of coupling leads to spin-dependent forces. They also show which type of coupling is associated with helicity-conservation. Needless to say that such information are essential in understanding the polarization phenomena in general, and its relationship to color-magnetic effects in particular.

IV Parametrization of effective potentials for large anlge elastic pp scattering.

Having discussed the general formalism (of our approach to pp in Section III) we now focus our attention on the polarization phenomena (mentioned in Section I). We present, in this framework, simple models which describe the large $p_\perp^2$-data. The need for studying such examples is not difficult to see: The observed relationship between the conceptually simplest polarization phenomenon[3,4,5,9] (namely the data on analyzing power in high-energy proton-proton elastic scattering) and the proposed picture[12] (in which rotating color charges in polarized hadrons manifest themselves in form of non-negligible color magnetic effects when the impact parameter between the colliding hadrons become very small compared with the average hadron size) should be put to further tests. In this connection, we asked ourselves the following question: " Is it possible to *quantify* this physical picture in such a way that not only the data on analyzing power, but also those on other characteristic features of this scattering process, can be described *quantitativly*? " The method we proposed for the description of such effects is similar to those used in Electrodynamics of macroscopic media and those in Nuclear Physics: We describe the effects due to the interactions between the constituents of different colliding hadrons macroscopically — *at the hadronic level* — in terms of effective potentials. Hence, the answer to this question is in the affirmative, provided that models can be explicitly constructed which lead to adequate descriptions of the data.

In constucting such models, it is important to keep the following points in mind:

(a) The relativistic kinematics for high-energy elastic proton-proton scattering allows in general the existence of five different types — namely the scalar-, the vector-, the tensor-, the axial vector- and the pseudoscalar-type of effective potentials. The question as to whether/how a given type contributes to the scattering process, depends not only on the interactions between the constituents (of the colliding protons) but also on the proton-structure. That is to say, a *derivation* of such effective potentials would be possible only if we could specify the above-mentioned intrinsic interactions and the proton structure explicitly.

(b) As we have seen in our analysis presented in Section III — especially through the illustrative examples — the characteristic features of the effective potentials depend very much on

their properties under Lorentz-transformation. While the coupling function $\bar{c}_\alpha(r)$ of the effective potentials $U_\alpha(x|i,j)$ $(\alpha = S,T,V,A,P)$ determines the strength and the range of $U_\alpha(x|i,j)$, it is *the corresponding bilinear covariants* which dictates the spin-dependence of the effective potential $U_\alpha(x|i,j)$.

(c) In order to take color-magnetic effects into account it is useful to consider the similarties and the differences between the color-magnetic and the electromagnetic forces. The latter suggests in particular that the vector-type coupling should play a dominant role. Furthermore, it can be readily shown (cf Section III) that the vector-type coupling yields in its non-relativistic limit the usual spin-orbit and the spin-spin interactions.

(d) As can be explicitly seen in the coupled integrodifferent equations (3.1) and (3.2), the effective potential obtained from a scalar-type coupling has the same kind of behaviour as the mass-term. This implies the existence of an intimate relationship between scalar-type coupling and helicity-nonconservation.

(e) As the non-relativistic limit explicitly shows, the tensor-type coupling implies the existence of a significant spin-spin interaction. Hence, the spin-spin correlation parameter A_{nn} is expected to depend considerably on the strength of the tensor-type effective potentials.

(f) High-energy elastic scattering can be, and has been described in terms of optical potentials.[26] They are complex potentials, the imaginary part of which guarantees the "absorption" of inelastic contributions.

(g) In those cases in which the coupling functions $\bar{c}_\alpha(r)(\alpha = \mathrm{S, V, T, A, P})$ has the functional form $exp(-\mu_\alpha r)/r$ where μ_α is a constant, the corresponding Fourier transform $\bar{g}_\alpha$ (as a function of invariant momentum transfer t or u) can be interpreated as the "propagator function" of an α-type meson of mass μ_α. This means, meson-exchange models which are suitable for high-energy elastic scattering processes and which incorporates such color effects can be taken as special examples of the proposed picture. Now, since a coupling function is nothing more than a possible phenomenological description of the strength and the range of the color-electric and color-magnetic forces,

there is apriori no reason why the coupling functions should have the form of Yukawa potentials where the masses of the known mesons are considered as fixed parameters.

(h) A simple and practical way to see whether, and (if yes) how much, the obtained result depends on the explicit form of the coupling functions is to follow the example of low-energy Nuclear Physics and study this question empirically. That is, comparison between results obtained from different kinds of Ansätze for the coupling function should be helpful.

In view of the foregoing considerations, we now discuss two possible models in which the coupling functions $\bar{c}_\alpha(r)$ are parametrized in the Gaussian form

$$\bar{c}_\alpha(r) = C^R_\alpha(r) + iC^I_\alpha(r), \qquad \alpha = S, T, V, A, P. \tag{4.1}$$

$$C^R_\alpha(r) = c_0(s) a^R_\alpha \exp\Big(-\frac{r^2}{4\lambda^2_{R\alpha}}\Big), \tag{4.2}$$

$$C^I_\alpha(r) = c_0(s) a^I_\alpha \exp\Big(-\frac{r^2}{4\lambda^2_{I\alpha}}\Big). \tag{4.3}$$

Here, $\lambda_{R\alpha}, \lambda_{I\alpha}, a^R_\alpha$ and a^I_α are real constants (in unit of GeV^{-1} and GeV respectively), while $c_0(s)$ is a (real) dimensionless function of s. In terms of this ansatz, the invariant amplitudes $f_\alpha(s,t,u)$ and $f_\alpha(s,u,t)$ can be readily obtained from Eqs. (3.17) - (3.20). The result is:

$$f^\epsilon_\alpha(s,t,u) = \kappa(s) a^\epsilon_\alpha \lambda^3_{\epsilon\alpha} \exp(-\lambda^2_{\epsilon\alpha}|t|) \tag{4.4}$$

$$f^\epsilon_\alpha(s,u,t) = \kappa(s) a^\epsilon_\alpha \lambda^3_{\epsilon\alpha} \exp(-\lambda^2_{\epsilon\alpha}|u|) \tag{4.5}$$

Here $\kappa(s) \equiv 8\pi^{3/2}\sqrt{2}c_0(s)$, and $\epsilon = R$ or I indicates the real and the imaginary part of f_α respectively. We note that, in terms of the parametrization of the coupling functions shown in Eqs. (4.1)-(4.3), the s-dependent coefficient $c_0(s)$ and thus $\kappa(s)$ cancels in the expressions for the quantities A and A_{nn}. The only place where it appears is in $d\sigma/dt$.

According to the analyses and the arguments presented at the end of Section III and in those given this section, the simplest model that has a chance to describe the striking features of the existing data is the following ansatz. We call it hereafter the SV-model. In this model: $\bar{c}_\alpha(r) \equiv 0$ for $\alpha = T, A, P$. The parameters of $\bar{c}_S(r)$ and $\bar{c}_V(r)$ in Eqs. (4.1) - (4.3) are in general different from zero. A set of parameter which approximately reproduce the $d\sigma/dt$, A and A_{nn} data are given in Table 3:

α	S		V	
ϵ	R	I	R	I
$a^\epsilon_\alpha[GeV]$	10	-7	-9	4
$\lambda^\epsilon_{\epsilon\alpha}[GeV^{-1}]$	0.7	0.9	0.8	0.7

Table 3

In the second example, which will be called hereafter the SVT-model, we set $\bar{c}_\alpha(r) \equiv 0$ for $\alpha = A, P$. The parameters for the coupling functions $\bar{c}_S(r), \bar{c}_V(r)$ and $\bar{c}_T(r)$ are given in Table 4

α	S		V		T	
ϵ	R	I	R	I	R	I
$a^\epsilon_\alpha[GeV]$	10	-10	-7	2	1	0
$\lambda^\epsilon_{\epsilon\alpha}[GeV^{-1}]$	0.7	1	0.8	0.7	0.7	0

Table 4

The result of this model is shown, together with the data in Figs. 1, 2, and 3. The similarities and the differences between the SV- and the SVT-model are shown in Figs. 5 and 6.

Other ways of parametrizing the coupling functions — in particular in Yukawa form — has also been considered in our numerical study. It turns out that the result depends very little on the particular form of the coupling functions; but in order to obtain nonvanishing polarization neither the scalar- nor the vector-effective potential should be identically zero.

It is interesting to see that the obtained numerical result confirms the expectations of our qualitative analysis: In order to understand the observed polarization phenomena at large momentum-transfer in terms of the proposed phenomenological approach of a QCD based picture, it is necessary to have scalar- and vector-effective potentials . (The inclusion of a tensor-effective potential improved the description of A_{nn}).

As next step, we wish to see whether/how the proposed picture can be used to describe the existing data in the medium- and the low- $p_\perp^2$ region. Furthermore, we also wish to see whether/how the proposed picture can be extended to other scattering processes. Of special interest are of course the striking phenomena observed in inclusive production of hyperons[27] and those of pions[28]. Studies along this line are now in progress.

Acknowledgement

We have benefited much from discussions with many colleagues — experimentalists and theorists. We wish to thank all of them, especially Chan Hong-mo, P. Kroll and Liang Zuo-tang.

References and Footnotes

1 See, for example, the articles in:

Proceedings of the Eigth International Symposium on High-Energy Spin Physics, Minneapolis, USA 1988, edited by K.J. Heller (AIP Conf. Proc. No. 187) (AIP, New York, 1989);

Proceedings of the Ninth International Symposium on High-Energy Spin Physics, Bonn, Germany 1990 (in press);

and the papers cited therein.

2 European Muon Collaboration: J. Ashman et al., Phys. Lett. B 206, 364 (1988).

3 See, for example, A. D. Krisch, in Proceedings of the Seventh International Symposium, Protvino, USSR, 1986, edited by L.D. Soloviev (Institute of High Energy Physics, Serpukhov, USSR, 1987), and the papers cited therein.

4 D.C. Peaslee et al., Phys. Rev. Lett. 51, 2359 (1983).

5 P.R. Cameron et al., Phys. Rev. D 32, 3070 (1985).

6 D.G. Crabb et al., Phys. Rev. Lett. **41**, 1257 (1978).

7 G.R. Court et al., Phys. Rev. Lett. **57**, 507 (1986).

8 D.G. Crabb et al., Phys. Rev. Lett. **60**, 2351 (1988).

9 A.D. Krisch, in Ref. 1 (1990).

10 See, for example, the comparisons between theories and experiments in Refs. 1, 3-9 and the papers cited therein.

11 See, for example,

R. Serber, Rev. Mod. Phys. **36**, 649 (1964)

G. Bellettini, in Proceedings of the 14th International Conference on High-Energy Physics, 1968, Vienna, Austria, ed. by J. Prentki and J. Steinberger, CERN (1968),

E. Segre, Nuclei and Particles, Benjamin/Cumming Pub. Co. Inc. (1977),

and the papers cited therein.

12 Liang Zuo-tang and Meng Ta-chung, Phys. Rev. **D42**, 1380 (1990).

13 Much of the ingredients of the proposed picture are already very old. The original papers and/or relevant review articles or books (which we can find) are cited in Ref. 12.

14 G. R. Farrar, in Ref. 1 (1988) Vol. 1 p. 112, and the references given therein.

15 See for example:

M.L. Goldberger et al. (GNO) Ann. of Phys. **2**, 226 (1957)

M.L. Goldberger et al. (GGMW) Phys. Rev. **120**, 2250 (1960)

E. Serber, Phys. Rev. Lett. **10**, 357 (1963)

D.H. Sharp and W.G. Wagner, Phys. Rev. **131**, 2226 (1963)

T.T. Wu and C.N. Yang, Phys. Rev. **137**, B708 (1965)

E. Leader, Rev. Mod. Phys. **39**, 663 (1967)

T.T. Chou and C.N. Yang, Phys. Rev. **170**, 1591 (1968)

H.D. Abarbanel, S.D. Drell and F.J. Gilman, Phys. Rev. Lett. **20**, 280 (1968)

L. Durand and R. Lipes, Phys. Rev. Lett. **20**, 637 (1968)

G.L. Kane and U.P. Sukhatme, Nucl. Phys. **B78**, 110 (1974)

A.J. Buras and J. Dias de Deus, Nucl. Phys. **B71**, 481 (1974)

T.T. Chou and C.N. Yang, Nucl. Phys. **B107**, 1 (1976)

L. Durand and F. Halzen, Nucl. Phys. **B104**, 317 (1976), Phys. Rev. **D15**, 352 (1977)

C. Bourrely, J. Soffer and T.T. Wu, Phys. Rev. **D19**, 3249 (1979)

S.J. Brodsky, C.E. Carlson and H. Lipkin, Phys. Rev. **D20**, 2278 (1979)

G.R. Farrar et al. , Phys. Rev. **D20**, 202 (1979)

G. Preparata and J. Soffer, Phys. Lett. **86B**, 304 (1979); and **93B**, 187 (1980)

C. Bourrely et al. Phys. Rep. **59C**, 95 (1980)

C. Bourrely and J. Soffer, Phys. Rev. Lett. **54**, 760 (1985)

J.A. Tjou and S.J. Wallace, Phys. Rev. **C32**, 1667 (1985), **C35**, 280 (1987)

S.M. Troshin and N.E. Tyurin, Int. J. of Mod. Phys. **5**, 2689 (1990).

16 We use the same normalization as Bourrely et al. Ref. 15 (1980).

17 See, for example, Eq. (2.9) in GNO (ref. 15) and Eq. (2.10) in GGMW (Ref. 15).

18 Due to our choice of normalization (See Footnote 16), this relation differs from that given in GGMW (Ref. 15, Eq. 4.2) by a factor $p/\sqrt{\pi}$.

19 See. for example, Eq. (2.6) in GGMW (Ref. 15).

20 See for example: L.I. Schiff, Quantum Mechanics (2nd Edition) Mc Graw-Hill (1955) p. 283.

21 See for example: J.D. Bjorken and S.D. Drell, Relativistic Quantum Mechanics, McGraw-Hill (1964).

22 This is similar with that used in the propagator theory. See e.g. Ref. 21: Eq. (7.1) on p. 100.

23 We note that according to the definition for $U_{0\alpha}(x|j,k)$, for $\alpha = S, V, T, A, P$, four term in the first rechtangle braket [ ] are equal to zero.

24 See, for example, GGMW (Ref. 15)

25 Compare, for example, this result with that for elastic electron-electron scattering given in Ref. 21.

26 See, for example: R. Serber (Refs. 11, 15), J.A. Tjou and S.J. Wallace (Ref. 15), and the papers cited therein.

27 See, for example, K. Heller, in Ref. 1 (1990); and the papers cited therein.

28 See, for example, A. Yokosawa, in Ref. 1 (1990) and the papers cited therein.

Figure Captions

1 Analyzing power A as function of $p_\perp^2$, wehre $p_\perp$ is the c.m.s. transverse momentum of the scattered proton. Data are taken from Refs. 4, 5 and 9. The curve is the result of the SVT-model.

2 Spin-correlation parameter A_{nn} as function of $p_\perp^2$. Data are taken from Refs. 6, 8 and 9. The curve is the result of the SVT model.

3 Differential cross-section $d\sigma/dt$ as function of $p_\perp^2$. Data are taken from Ref. 11. The curves are the results of the SVT model. The s-dependent parameter $\kappa(s)$ is 0.4 and 0.2 for $p_{lab} = 12$ and 24 GeV/c respectively.

4 Diagrams for elastic proton-proton scattering. The quantum number (p_1^i, λ_1^i), (p_2^i, λ_2^i), $(p_1^f \lambda_1^f)$, $(p_2^f \lambda_2^f)$ indicate the plane-wave solutions in the initial and the final states respectively.

5 Analyzing power A as function of $p_\perp^2$. Comparison between the SV and SVT-model.

6 Spin correlation parameter A_{nn} as function of $p_\perp^2$. Comparison between the SV- and the SVT-model.

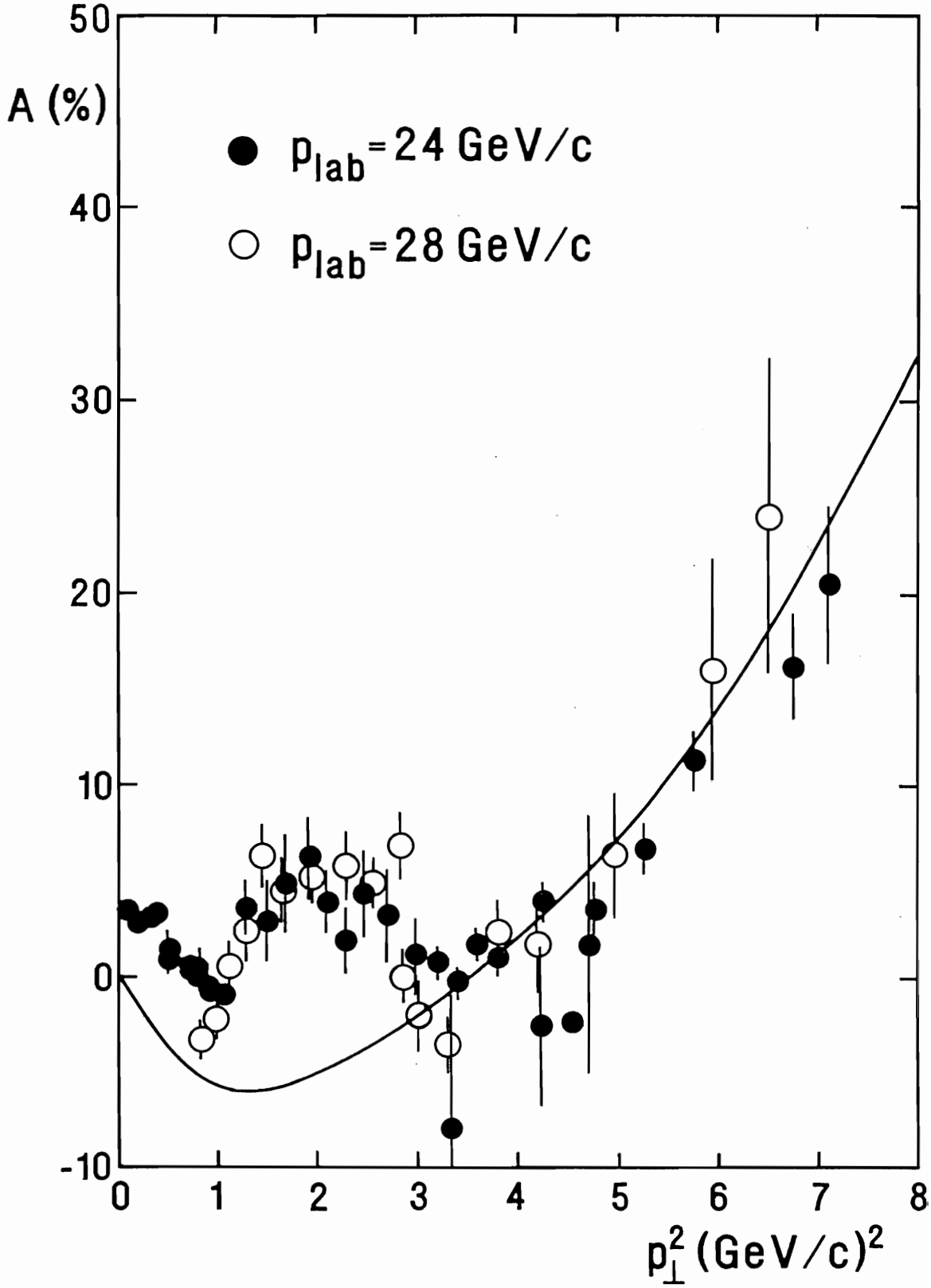
A (%)
50
40
30
20
10
0
-10
p_{lab}=24 GeV/c
p_{lab}=28 GeV/c
0
1
2
3
4
5
6
7
8
$p_\perp^2$ (GeV/c)^2

Fig.1

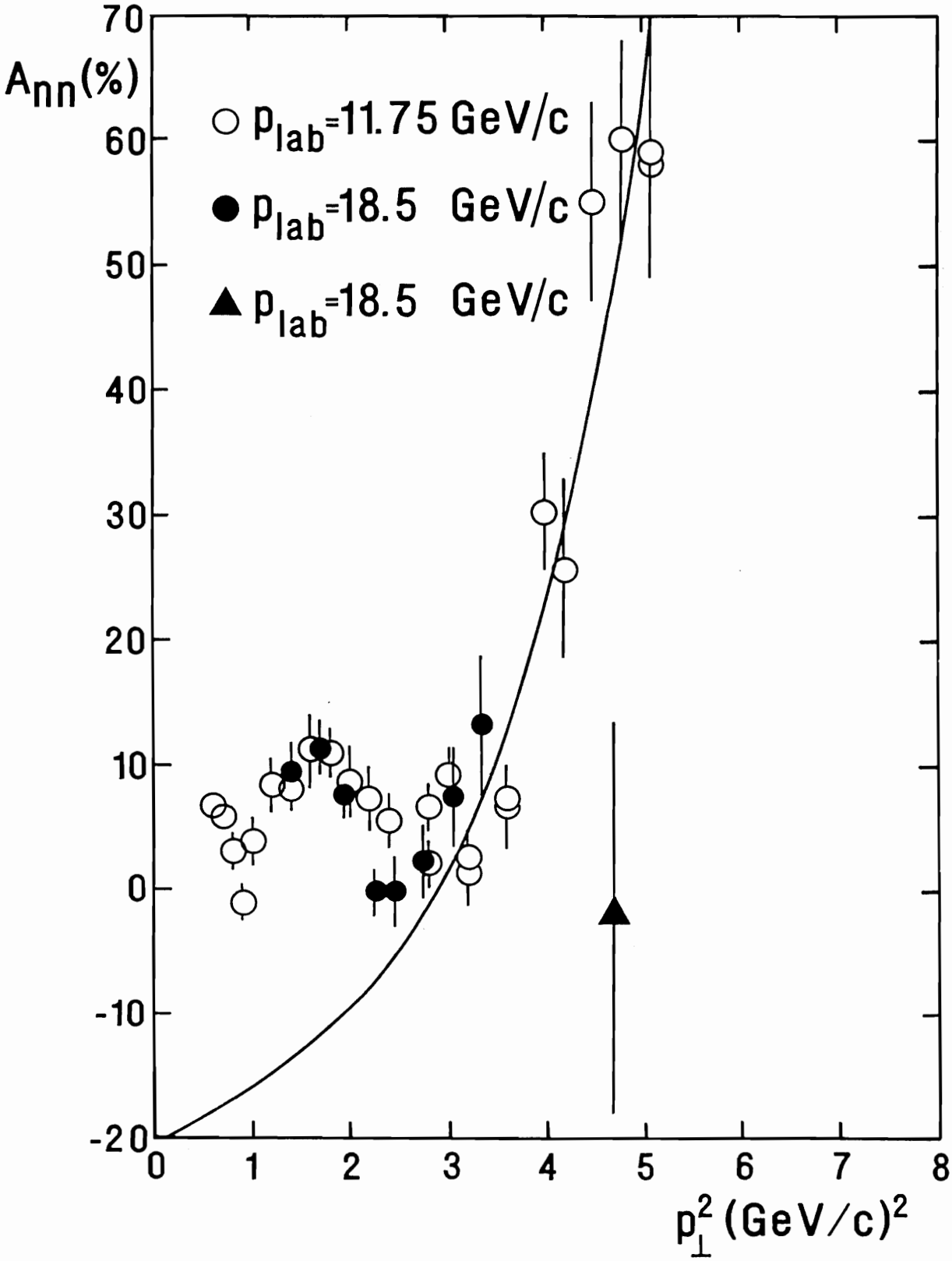
A_{nn}(%)
70
60
50
40
30
20
10
0
-10
-20
○ p_{lab}=11.75 GeV/c
● p_{lab}=18.5 GeV/c
▲ p_{lab}=18.5 GeV/c
0
1
2
3
4
5
6
7
8
$p_\perp^2$ (GeV/c)^2

Fig.2

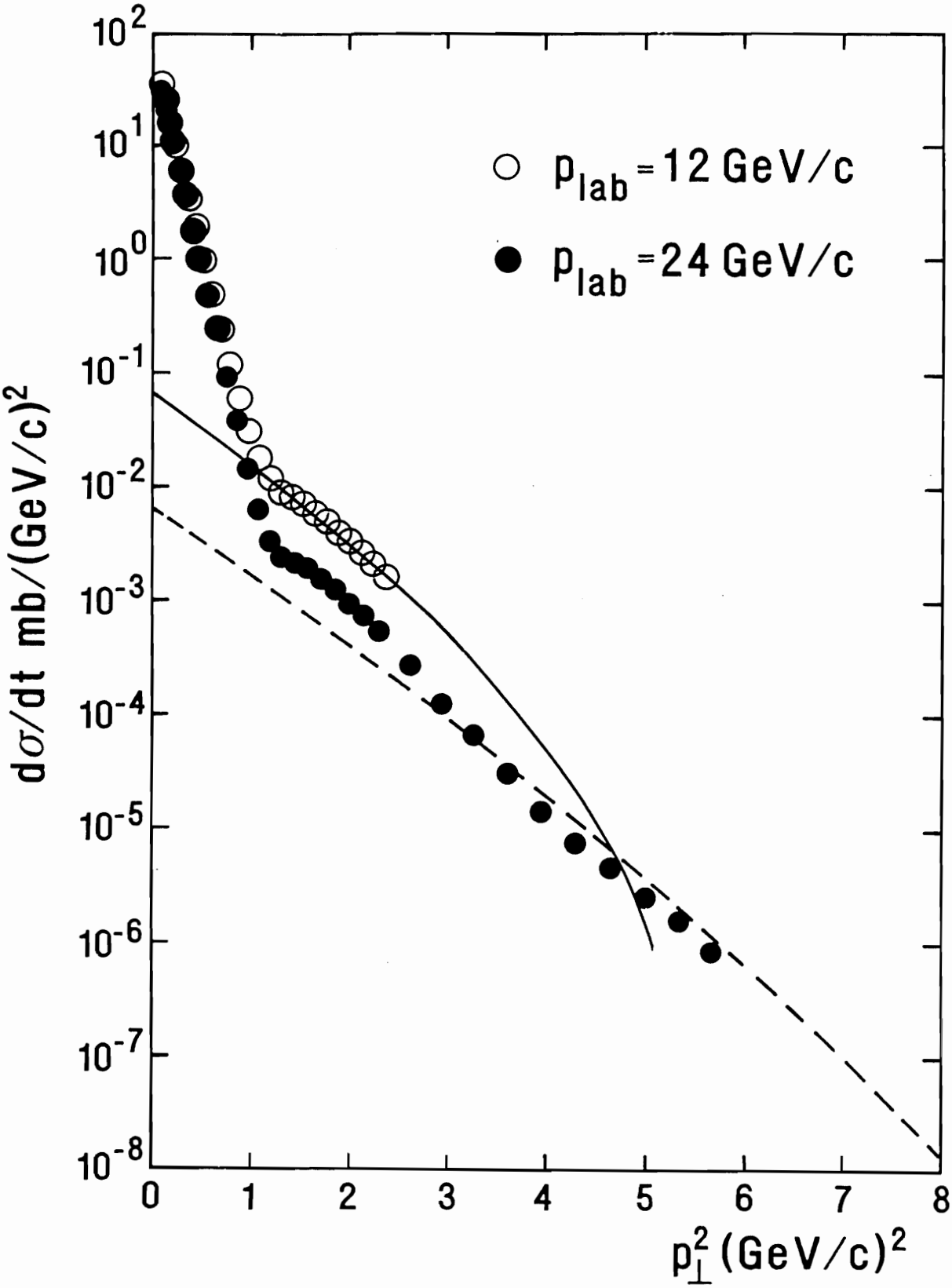
10^2
10^1
10^0
10^{-1}
10^{-2}
10^{-3}
10^{-4}
10^{-5}
10^{-6}
10^{-7}
10^{-8}
$d\sigma/dt$ mb/(GeV/c)^2
p_{lab} = 12 GeV/c
p_{lab} = 24 GeV/c
0
1
2
3
4
5
6
7
8
$p_\perp^2$ (GeV/c)^2

Fig.3

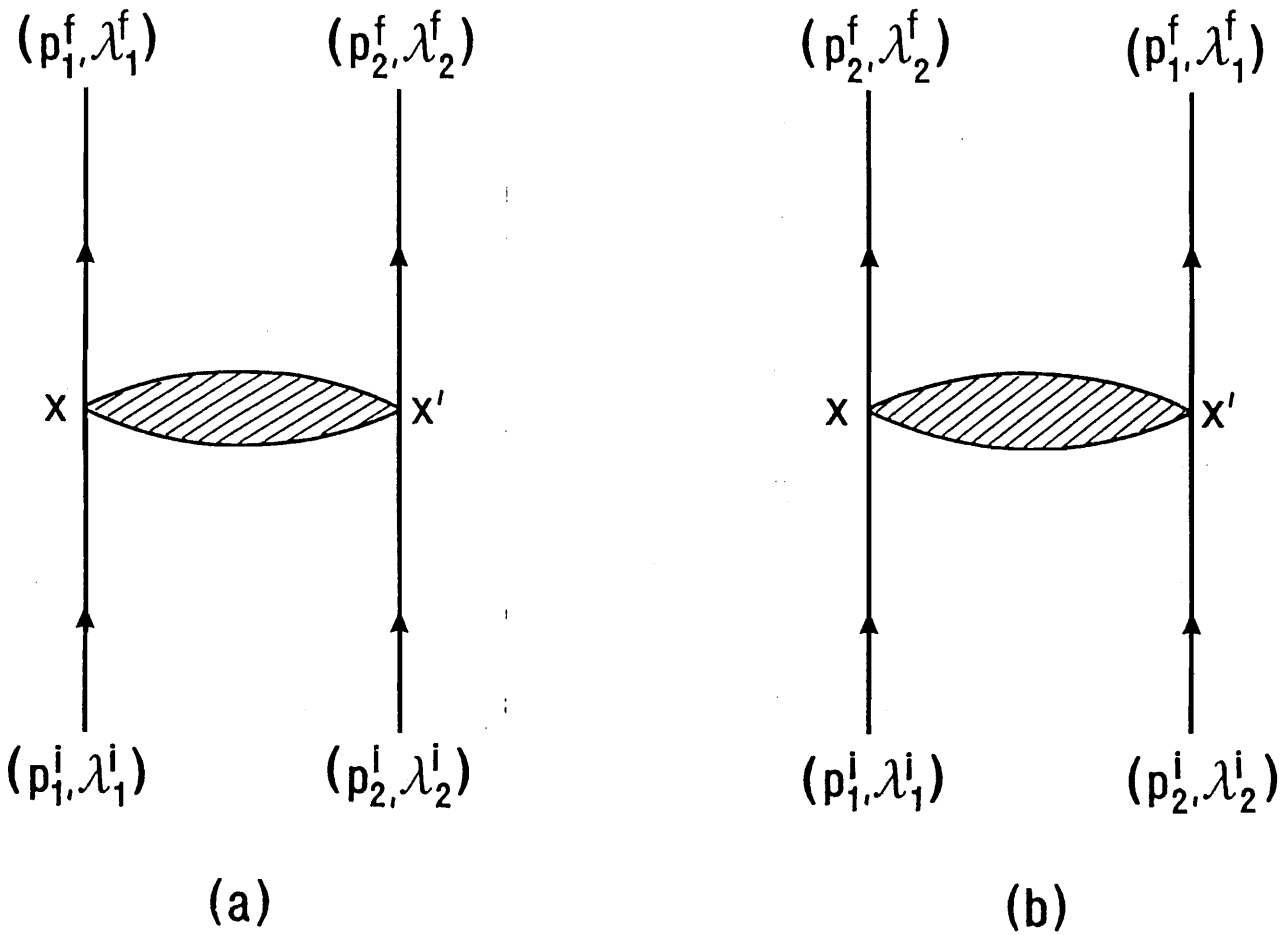
(p_1^f, λ_1^f)
(p_2^f, λ_2^f)
x
x′
(p_1^i, λ_1^i)
(p_2^i, λ_2^i)
(a)
(p_2^f, λ_2^f)
(p_1^f, λ_1^f)
x
x′
(p_1^i, λ_1^i)
(p_2^i, λ_2^i)
(b)

Fig. 4

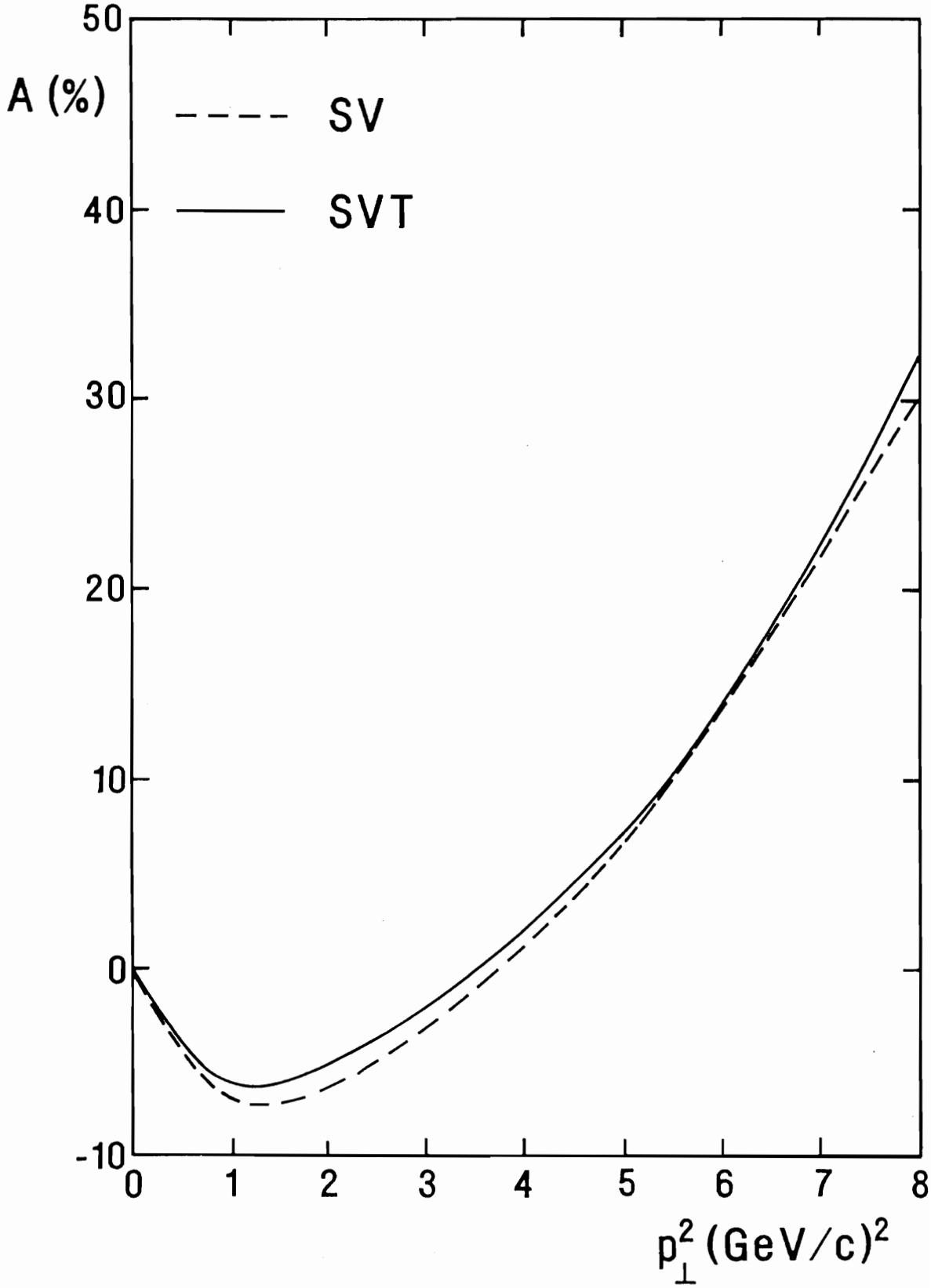

Fig.5

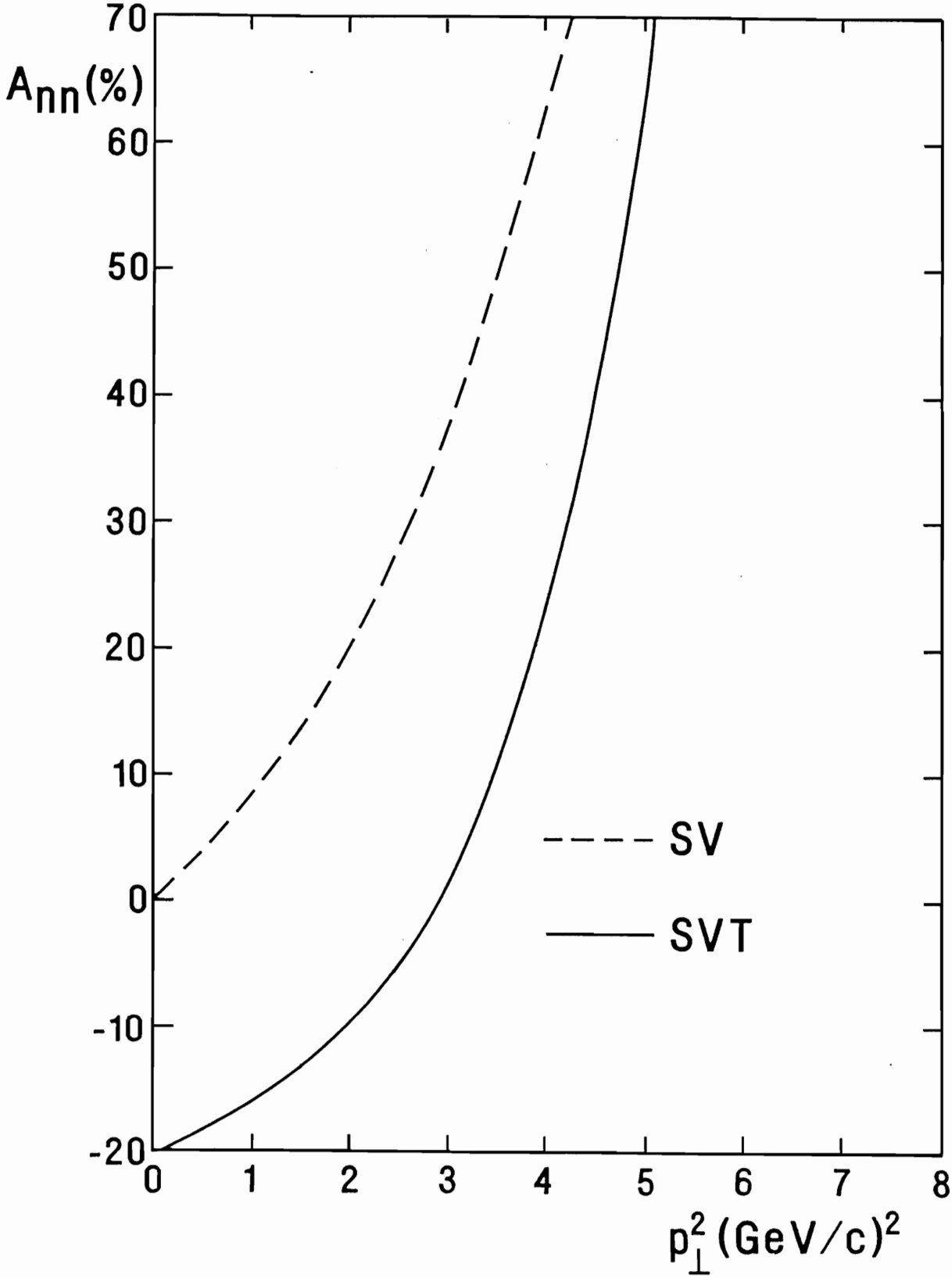

Fig.6